

센서 응답의 Time-Profile 을 이용한 전자 후각 (E-Nose) 시스템의 Vapor 인식 성능 향상

양윤석

한국전자통신연구원 기반기술연구소 바이오소자팀
(2004년 7월 23일 접수, 2004년 8월 9일 채택)

Improved Vapor Recognition in Electronic Nose (E-Nose) System by Using the Time-Profile of Sensor Array Response

Yoon Seok Yang

Bio-MEMS Team, Basic Research Laboratory, Electronics and Telecommunications Research Institute (ETRI),
(Received July 23, 2004. Accepted August 9, 2004)

요 약 : 전자 후각 (E-nose) 시스템은, 전통적으로 음식물이나 플라스틱 제재의 생산에서 자동화된 품질관리 시스템에 사용되어 왔으나, 최근 호흡가스 등을 통해 당뇨, 호흡 및 소화기 질환과 감염 등을 검사하는 진단영역으로 그 응용분야를 확대하고 있다. 이러한 질병과 연관이 있는 휘발성 유기화합물 (volatile organic compound, VOC) 에 대하여 E-nose 의 센서어레이는 센서 물질과 휘발성 화합물 사이의 반응으로 인해 고유한 반응을 보이며, 신호의 profile 에 그 흔적을 남긴다. 본 연구에서는 센서어레이의 반응 신호를 profile 형태로 유지 및 분석함으로써 E-nose 의 가스시료 인식 성능을 보다 향상시킬 수 있는 방법을 제안하였다. 신호의 profile 에는 패턴인식을 위한 기존의 개별적인 특성 (feature) 보다 많은 정보가 들어 있으며, 이를 가스의 구분에 효과적으로 이용하기 위해 디지털 영상처리에서 사용되는 패턴 매칭을 응용한 time-profile 방법을 새롭게 제안하였다. 제안된 방법의 검증을 위해, 반도체 공정에 의해 제작된 16 채널의 초소형 가스센서 어레이를 사용해 측정된 8 종류의 각기 다른 가스시료들에 대하여, 동종 및 이종 가스간의 매칭의 정도를 산출하였다. 기존의 방법과 비교한 결과 동종과 이종 가스간의 뚜렷한 구별이 가능하여 이를 패턴인식에 사용하면 E-nose 의 가스 인식 성능을 향상시킬 것으로 전망된다.

Abstract : The electronic nose (E-nose) recently finds its applications in medical diagnosis, specifically on detection of diabetes, pulmonary or gastrointestinal problem, or infections by examining odors in the breath or tissues with its odor characterizing ability. The odor recognition performance of E-nose can be improved by manipulating the sensor array responses of vapors in time-profile forms. The different chemical interactions between the sensor materials and the volatile organic compounds (VOC's) leave unique marks in the signal profiles giving more information than collection of the conventional piecemeal features, i.e., maximum sensitivity, signal slopes, rising time. In this study, to use them in vapor recognition task conveniently, a novel time-profile method was proposed, which is adopted from digital image pattern matching. The degrees of matching between 8 different vapors were evaluated by using the proposed method. The test vapors are measured by the silicon-based gas sensor array with 16 CB-polymer composites installed in membrane structure. The results by the proposed method showed clear discrimination of vapor species than by the conventional method.

Key words : Electronic nose (E-nose), Medical diagnosis, Volatile organic compound (VOC), Vapor recognition, Pattern matching, Response profile, Gas sensor array

INTRODUCTION

The electronic nose (E-nose) system has been mainly used in food industry where it reduces the amount of the analytical

chemistry, i.e., inspection of food quality, control of cooking process, and checking odors plastic packaging, etc. due to its ability of characterizing odors, vapors, and gases [1]. Recently, various composites from carbon-black (CB) and organic polymers are developed as gas sensors for portable use due to its chemical diversity by the selection of proper organic polymers and improved operability with lower power consumption than the metal oxide gas sensors [2,3]. With the help of these improvements in portability and ease of use, the E-nose is widening its potentials in environmental and pollution monitoring i.e., real-time identification of contaminants, analysis of fuel mixture, detection of oil leaks, testing ground water for odors, and identification of toxic waste, etc. And it also finds its

This work has been supported in part by the Ministry of Information and Communication of Korea and in part by the Ministry of Science and Technology of Korea through the NRL program.

통신저자 : Yoon Seok Yang, Ph.D.

Bio-MEMS Team, Basic Research Laboratory,
Electronics and Telecommunications Research Institute (ETRI),

161 Gajeong-dong, Yuseong-gu,

Daejeon, 305-350, KOREA

Tel : 8242-860-1471 Fax : 8242-860-6836

E-mail : lucid@etri.re.kr

applications in medical diagnosis, specifically on detection of diabetes, pulmonary or gastrointestinal problem, or infections by examining odors in the breath or tissues [4,5]. The presence of some volatile compounds is associated to those diseases. For example, mercaptans and aliphatic acids were found in the breath of patients with liver cirrhosis [6], and dimethyl- and trimethylamine were found in the breath of uremic patients [7]. Some alkanes (hexane and methylpentane among the others) and benzene derivatives such as o-toluidine and aniline observed in affected individuals have been claimed to be correlated to the lung cancer [8].

The volatile compounds show unique response signals in their magnitudes and shapes, so that the patterns gathered from the sensor array help the artificial intelligence algorithm to recognize the vapors automatically. In case of chemi-resistive gas sensor array system, the most commonly used feature describing the pattern is the maximum sensitivity [2]. It is defined by the maximum ratio of resistance change induced by the inhaled vapors [2]. And several shape-related features such as signal slopes, rising-time, etc. are used together to improve the vapor identification rate in pattern recognition algorithm. Additionally, many statistical techniques are applied to differentiate the vapors based on these features [2]. However, when we identify the vapors based on the maximum sensitivities, there are unexpected overlaps between different vapor species. Additional parameters taken to compensate for these errors need sophisticated algorithms to extract from noisy signals. They depend more on the characteristics of gas flow unit in the system than on the interaction characteristics between the vapor and the sensor materials. They are thought to be fragmentary, that is, it is hard to maintain the consistencies among them when surrounding conditions are varied.

Since the E-nose basically responds to wide range of volatile compounds, it is no more important to develop sensor arrays showing high selectivity for various vapors than to make full use of the sensor-array response in recognizing target vapors [2]. There are much more information in the time-profiles of the sensor array response itself, each of which is the vivid record of the unique interaction between the organic polymer composites and the incoming vapor. Therefore, this paper proposes a new algorithm to utilize the time response of the sensor array exposed to vapors in way that is more natural. It keeps the whole profile records of the sensor array time-responses and compares them with one another quantitatively by adopting a correlation-based image pattern matching method. The proposed methods were verified with 8 different vapor species and the 16 channel sensor array. The identification of the basic volatile organic compounds (VOC's) is a necessary step prior to the recognition of the volatile pattern of their mixtures, which is more realistic and complicated.

SENSOR ARRAY AND MEASUREMENT OF THE VAPOR RESPONSE

The sensor array was implemented by dispensing the CB-polymer composite-solvent solution in the micromachined gas sensor array chip in figure 1. It consists of 16 separate sensors with an interdigitated electrode, microheater, and micromachined membrane in each channel for further temperature-controlled measurement applications. The 16 CB polymer composites are described in table 1. The resistive sensors are interfaced with the instrumentation circuitry including voltage divider, amplifier, and low-pass filter. The measured data are collected in PC using data acquisition (DAQ) board DAQ6062E and LabVIEW (National Instrumentation, USA). The voltage-diver operated in the range from 10 to +10 volts and gains of 16 identical amplifiers were set to 10 (output/input voltage) for maximum DAQ resolution.

The proposed method was applied to 8 different vapor species (acetone, benzene, cyclo-hexane, ethanol, heptane, methanol, propanol, toluene). Each vapor was measured 20 times using the sensor array [9], as pictured in figure 1 yielding 160 time-profile total. The flow control unit in our system allows the vapors to flow in at desired concentration during about 60 seconds, and afterward flushes the remainder by air flow for about 2 minutes. The chemi-resistive sensor array undergoes resistance change upon exposure to vapor and succeeding air flow. It shows typical response signal in figure 2. The rising voltages imply the increased resistances, and the falling voltages correspond to the decreased resistances. The measured data are handled by MATLAB (Mathworks, USA) on Pentium IV PC.

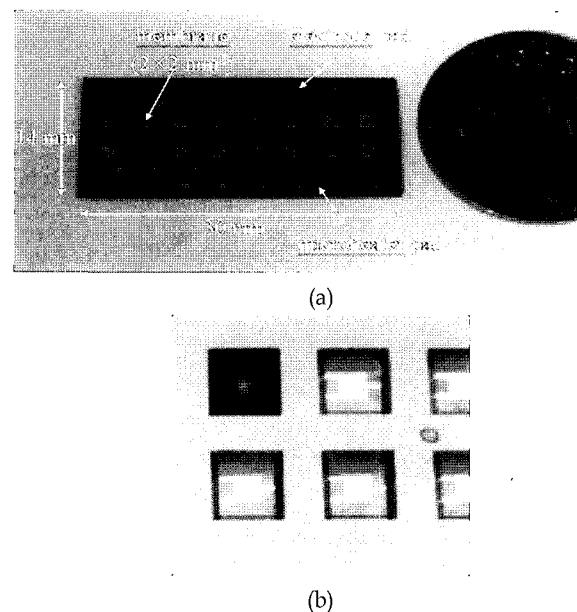


Fig. 1. Photograph of gas sensor array chip. (a) its physical dimensions and 16 separate sensing channels with an interdigitated electrode, microheater, and micromachined membrane well, and (b) CB polymer composites sensor built inside of the micromachined well

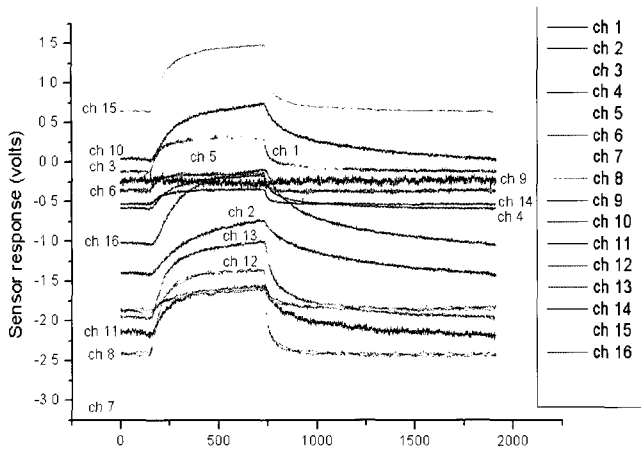


Fig. 2. Typical time-responses of 16 channel sensor array with respect to inflow of acetone vapor at 5000 ppm

Table 1. The list of 16 CB polymer composites used in Si-based sensor array

Ch 1	poly(methyl methacrylate)
Ch 2	polyvinylpyrrolidone
Ch 3	poly(vinyl acetate)
Ch 4	poly(ethylene oxide)
Ch 5	polycaprolactone
Ch 6	poly(4-methylstyrene)
Ch 7	poly(styrene-co-methyl methacrylate)
Ch 8	poly(ethylene-co-vinyl acetate)
Ch 9	poly(Bisphenol A Carbonate)
Ch 10	poly(4-vinyl pyridine)
Ch 11	poly(vinyl butyral)-co-vinyl alcohol-co-vinyl acetate
Ch 12	poly(vinyl stearate)
Ch 13	Ethyl cellulose
Ch 14	polystyrene-black-polyisoprene-black-polystyrene
Ch 15	hydroxypropyl cellulose
Ch 16	cellulose acetate

No.Polymer I.D.

MULTI-CHANNEL PROFILES

As stated previously, figure 2 contains the detailed records of the interactions between the sensor materials and the incoming vapors. The records are slightly different according to the vapors. These subtle differences can be observed effectively by combining the multi-channel signals together. For visual example, the 3rd channel response versus the 4th channel response is plotted in figure 3. It

makes interesting trajectory on 2-dimensional space with respect to a vapor inflow and outflow. All of the 160 responses from the 8 vapor species are traced in the same manner and are shown in figure 4. Each has 20 identical circulated response trajectories with slight offsets due to the baseline-shift between repeated measurements. Every vapor has its own trajectory pattern distinguished from one another. Heuristically, it is thought that the differences in their patterns become more significant as more channels participate in traces together. Equation (1) defines the multi-channel profiles in vector form.

$$P^n(t) = \begin{bmatrix} p_1(t) \\ p_2(t) \\ \vdots \\ p_n(t) \end{bmatrix} \quad (1)$$

$p_n(t)$: response profiles of nth sensor channel.
 $P^n(t)$: n-dimensional response profile in a vector form.

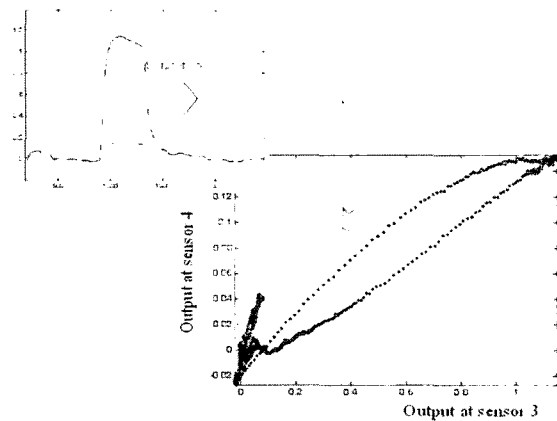


Fig. 3. A typical plot of the combined response profiles. (x, y) positions in the right graph are correspond to the values of (channel 3, channel 4) in the left graph

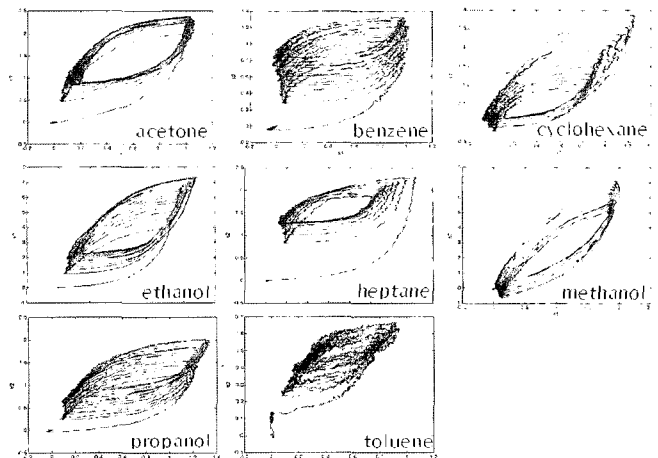


Fig. 4. 8 basic vapors show various combined profiles in 2-dimensional space. As in the figure 3, the horizontal and vertical axis correspond to the magnitude of response at sensor 3 and 4, respectively

Figure 5 shows an exemplar trace of P3(t) in classification space to make the patterns clear in the vapor recognition view point. The clustering results for the same vapor set using the conventional maximum sensitivities are shown in figure 6 for comparison. The patterns in figure 5 are more easily and clearly identified than those in figure 6 owing to the detailed records of the chemical reaction on the vapor sensors. Therefore, it can reduce the errors in vapor recognition if these trajectory or curvature patterns are properly differentiated.

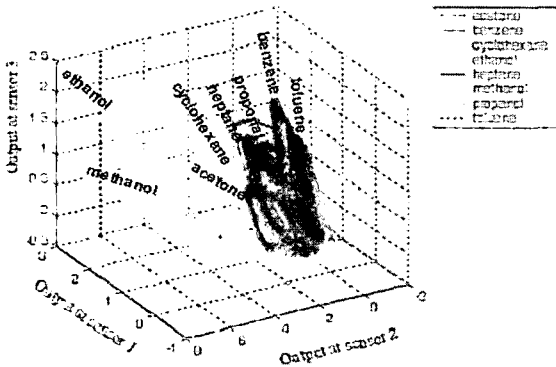


Fig.5. Vapor clustering results by the multi-channel profiles (x-y-z axes correspond to sensor 1, sensor 2, sensor 3, respectively)

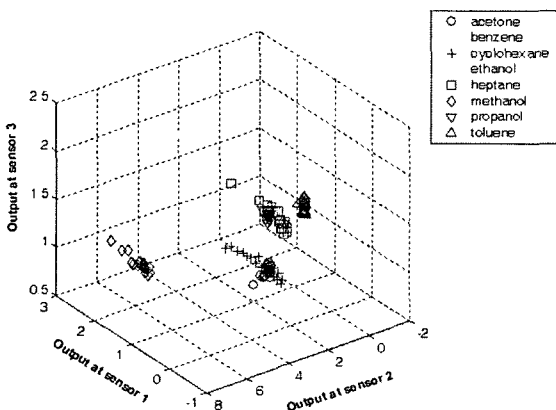


Fig 6. Vapor clustering results by the conventional maximum sensitivities

PATTERN MATCHING

Though there are many complicated ways to describe quantitatively the curvatures for differentiation, such patterns can be clustered easily with refer to the measure-of-similarity's among them. The P16(t)'s of vapors are associated with intensity-mapped pictures as in figure 7. The properties of profiles are reserved in intensity patterns of the image. Then the measure-of-similarity's between any two vapors are simply evaluated by correlation-based image pattern matching algorithm defined by (2). Equation (2) has a value between 1 and +1, and becomes large as the similarity

between x and y increases. It equals to -1 when x and y are negatively identical, and equals to 1 when x and y are positively identical. For computation, all the vapor images were maintained equal in their sizes by controlling the time for signal measurement and were slightly adjusted before the computation if necessary.

$$\text{Corr. coef}_{xy} = \frac{\sigma_{xy}^2}{\sigma_x \sigma_y} \quad (2)$$

x and y: intensity values of two vapor images, respectively.
xy: covariance of x and y.
x, and y: standard deviation of x and y, respectively.

This clustering method is more robust than the conventional piecemeal-feature extraction method. Most of feature extraction algorithms are suffering from the distortions by noisy interference and artifacts, i.e., unexpected fluctuation in vapor flow or temperature changes, etc. To the contrary, since it belongs to statistic methodology, the correlation-based matching score diminishes the unexpected artifacts or the noisy interferences.

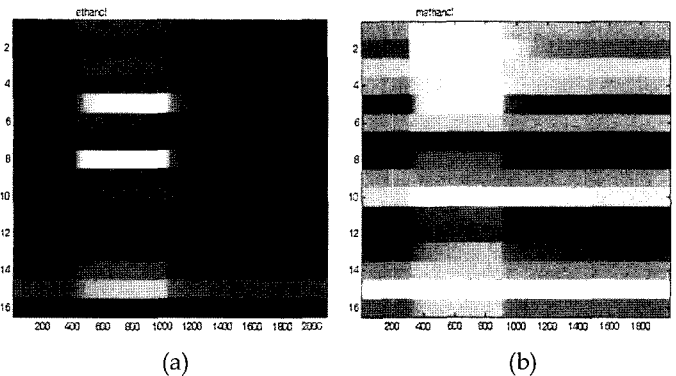


Fig 7. Images associated with the multi-channel profiles of (a) ethanol, (b) methanol. The horizontal axis corresponds to the time index, and the vertical labels imply the channel index.

RESULTS AND DISCUSSION

The pattern matching scores among 8 different vapor species evaluated by the proposed methods are shown in table 2. As can be seen in the table, there are 64 cases of pairing 2 vapor species for pattern matching. In each case, both vapors have 20 repeated measurements, and hence 400 matching scores. Each value in table 2 is their average. The scores using the conventional maximum sensitivities as shown in figure 9 are also evaluated in table 3 for comparison. Table 2 shows significantly higher contrast between the same (on-diagonal positions) and different (off-diagonal positions) vapor species than table 3. Figure 8 and figure 9 show the same results in intensity-mapped

image formats with emphasis on the figure 8's significant enhancements in gray level differences between matching vapors and non-matching vapors. When implemented in real system, the higher contrast in table 2 helps the E-nose system to set definite thresholds to cut off the non-matching samples in vapor identification

Though the horizontal size of the images (length of time-responses) is about 2000 data points which seems to be large, the amount of computation is at most comparable to the multi-layer neural network implementation taking signal descriptive features as inputs. Actually, the computation for a single matching score needs less than 1 second by MATLAB on Pentium IV PC. Moreover, the complexity in the evaluation of the matching scores is not so high as that in the conventional piecemeal feature extraction. The conventional feature extractions such as finding the maximum point, computing the slopes, estimating the rising-times up to maximum value or back to baseline level, etc. need some sophisticated data manipulations. And they are affected more severely by the vapor flow condition of the system than by the interaction between sensors and vapors. These effects are difficult to compensate by algorithms. The correlation-based pattern matching is robust to these annoying effects as stated previously, and the changes in the flow control are simply compensated by adjusting the horizontal size of the vapor images to the pre-defined target pictures. These pictures can be made up simply by keeping some typical responses of the target vapors. There is no need to analyze the signals to obtain any characteristic parameters.

By the way, the flow effects are canceled out by combining the multi-channel values into a curvature as in figure 3. It shows consequently only the relative differences in the activities of sensing materials in response to the incoming vapor. This kind of relative quantity is so useful in the application fields of automatic pattern recognition or machine intelligence because it can exclude the need for extra adjustment or calibration caused by changes in flow units or surrounding conditions. It is necessary to explore new methods to use the information in the curvatures. Additionally, the time-profile method seems to be lossless, from the information point of views, since it reserves the whole record of the vapor measurement signals. Excluding the power-line interferences, the random fluctuations overall in the measured profiles are thought to be one of the informative properties of the vapor response signals. Some advanced image-based techniques such as texture or histogram analysis are known to be able to define significant patterns in such random components. They will be adopted in further study to enhance the robustness and accuracy of the vapor recognition algorithms.

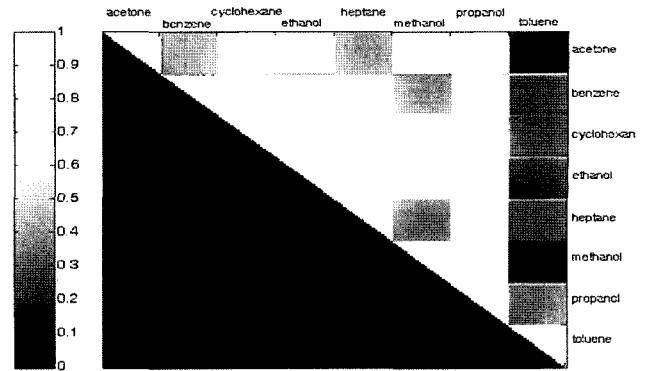


Fig 8. Intensity level representation of the matching scores in table 2.

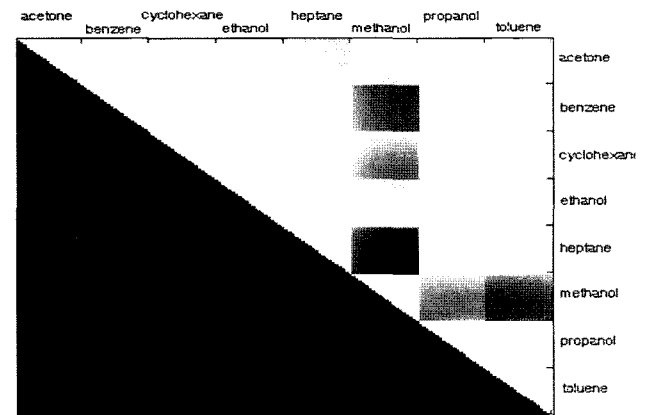


Fig 9. Intensity level representation of the matching scores in table 3.

CONCLUSIONS

The results verified that the correlation-based pattern matching with the multi-channel response profiles is able to classify the vapor species based on the evaluated scores. Therefore, it can be concluded that the proposed time-profile method is expected to improve the vapor recognition in E-nose, if it once has some pre-defined pictures of the target vapor profiles. Likewise, the proposed method can be applied to the pattern recognition of the VOC mixtures in realistic situations.

Now, the E-nose in this study is being developed in portable form with miniaturized electronics. This will help the on-site acquisition and test of the breath samples and consequently will make it possible to use the E-nose on the point-of-care-testing (POCT) in medical applications.

Table 2. Matching scores by 16-channel profiles between 8 vapor species. Each value is an average of 400 possible pairs between 20 repeated measurement for 2 vapors, respectively.

	acetone	benzene	cyclo -hexane	ethanol	heptane	methanol	propanol	toluene
acetone	0.996	0.468	0.839	0.654	0.449	0.921	0.746	0.145
benzene	-	0.930	0.750	0.835	0.903	0.422	0.845	0.315
cyclo -hexane	-	-	0.990	0.878	0.754	0.802	0.942	0.306
ethanol	-	-	-	0.977	0.757	0.692	0.934	0.260
heptane	-	-	-	-	0.974	0.406	0.801	0.322
methanol	-	-	-	-	-	0.990	0.691	0.031
propanol	-	-	-	-	-	-	0.993	0.407
toluene	-	-	-	-	-	-	-	0.995

Table 3. Matching scores for the same vapor measurements by the conventional maximum sensitivities

	acetone	benzene	cyclo -hexane	ethanol	heptane	methanol	propanol	toluene
acetone	0.995	0.781	0.829	0.945	0.595	0.650	0.903	0.795
benzene	-	0.997	0.959	0.845	0.927	0.278	0.944	0.995
cyclo -hexane	-	-	0.980	0.889	0.914	0.452	0.934	0.949
ethanol	-	-	-	0.995	0.673	0.673	0.953	0.858
heptane	-	-	-	-	0.998	0.165	0.793	0.899
methanol	-	-	-	-	-	0.993	0.448	0.282
propanol	-	-	-	-	-	-	1.000	0.957
toluene	-	-	-	-	-	-	-	1.000

REFERENCES

1. T. C. Pearce, S. S. Schffman, H. T. Nagle, and J. W. Gardner, *Handbook of machine olfaction*, Weinheim, Wiley-Vch, 2003
2. B. J. Doleman, M. C. Lonergan, E. J. Severin, T. P. Vaid, and N. S. Lewis, "Quantitative study of the resolving power of arrays of carbon black-polymer composites in various vapor-sensing tasks", *Anal. Chem.*, Vol. 70, pp. 4177-4190, 1998
3. Y. Mo, Y. Okawa, K. Inoue, and K. Natukawa, "Low-voltage and low-power optimization of micro-heater and its on-chip drive circuitry for gas sensor array", *Sens. Actuators A Phys.*, Vol. 100, pp. 94-101, 2002
4. C. D. Natale, A. Macagnano, E. Martinelli, R. Paolesse, G. D' Arcangelo, C. Roscioni, A. Finazzi-Agrò, and A. D' Amico, "Lung cancer identification by the analysis of breath by means of an array of non-selective gas sensors", *Biosensors and Bioelectronics*, Vol. 18, pp. 1209-1218, 2003
5. J. W. Gardner, H. W. Shin, and E. L. Hines, "An electronic nose system to diagnose illness", *Sensors and Actuators B Chem.*, Vol. 70, pp. 19-24, 2000
6. H. Kaji, M. Hisamura, N. Sato, and M. Murao, "Evaluation of volatile sulfur compounds in the expired alveolar gas in gas patients with liver cirrhosis", *Clinical Chimica Acta.*, Vol. 85, pp. 279-284, 1978
7. M. Simenhoff, J. Burke, L. Saukkonen, A. Ordinario, and R. Doty, "Biochemical profile of uremic breath", *New England Journal of Medicine*, Vol. 297, pp. 132-135, 1977
8. H. J. O'Neil, S. M. Gordon, M. H. O'Neil, R. D. Gibbons, and J. P. Szidon, "A computerized classification technique for screening for the presence of breath biomarkers in lung cancer", *Clinical Chemistry*, Vol. 34, pp. 1613-1618, 1988
9. S. Ha, Y. S. Kim, Y. Yang, Y. J. Kim, S. Cho, H. Yang, and Y. T. Kim, "Integrated and microheater embedded gas sensor array based on the polymer composites dispensed in micromachined wells", *Sensors and Actuators B Chem.*, in press